Biochimica et Biophysica Acta 1832 (2013) 2302–2314

Contents lists available at ScienceDirect

Biochimica et Biophysica Acta

journal homepage: www.elsevier.com/locate/bbadis

Transthyretin suppresses the toxicity of oligomers formed by misfolded proteins in vitro

Roberta Cascella [a], Simona Conti [a], Benedetta Mannini [a], Xinyi Li [b], Joel N. Buxbaum [b], Bruno Tiribilli [c], Fabrizio Chiti [a], Cristina Cecchi [a,*]

[a] Department of Biomedical Experimental and Clinical Sciences, University of Florence, V.le GB Morgagni 50, 50134 Florence, Italy
[b] Department of Molecular and Experimental Medicine, The Scripps Research Institute, La Jolla, CA 92037, USA
[c] Consiglio Nazionale delle Ricerche (CNR), Istituto dei Sistemi Complessi, Via Madonna del Piano 10, 50019 Sesto Fiorentino, Florence, Italy

ARTICLE INFO

Article history:
Received 14 May 2013
Received in revised form 16 September 2013
Accepted 18 September 2013
Available online 25 September 2013

Keywords:
Molecular chaperone
TTR protective effect
TTR-mediated oligomer clustering

ABSTRACT

Although human transthyretin (TTR) is associated with systemic amyloidoses, an anti-amyloidogenic effect that prevents Aβ fibril formation in vitro and in animal models has been observed. Here we studied the ability of three different types of TTR, namely human tetramers (hTTR), mouse tetramers (muTTR) and an engineered monomer of the human protein (M-TTR), to suppress the toxicity of oligomers formed by two different amyloidogenic peptides/proteins (HypF-N and $A\beta_{42}$). muTTR is the most stable homotetramer, hTTR can dissociate into partially unfolded monomers, whereas M-TTR maintains a monomeric state. Preformed toxic HypF-N and $A\beta_{42}$ oligomers were incubated in the presence of each TTR then added to cell culture media. hTTR, and to a greater extent M-TTR, were found to protect human neuroblastoma cells and rat primary neurons against oligomer-induced toxicity, whereas muTTR had no protective effect. The thioflavin T assay and site-directed labeling experiments using pyrene ruled out disaggregation and structural reorganization within the discrete oligomers following incubation with TTRs, while confocal microscopy, SDS-PAGE, and intrinsic fluorescence measurements indicated tight binding between oligomers and hTTR, particularly M-TTR. Moreover, atomic force microscopy (AFM), light scattering and turbidimetry analyses indicated that larger assemblies of oligomers are formed in the presence of M-TTR and, to a lesser extent, with hTTR. Overall, the data suggest a generic capacity of TTR to efficiently neutralize the toxicity of oligomers formed by misfolded proteins and reveal that such neutralization occurs through a mechanism of TTR-mediated assembly of protein oligomers into larger species, with an efficiency that correlates inversely with TTR tetramer stability.

1. Introduction

Transthyretin (TTR) is a homotetrameric protein with a total molecular mass of 55 kDa that was originally thought to be synthesized only in the liver, choroid plexus of the brain, and retina [1,2]. Further studies have demonstrated significant and perhaps physiologically important synthesis in the pancreas, kidneys, Schwann cells and neurons [3–7]. In the plasma TTR transports thyroxine (T_4) and the retinol binding protein charged with retinol (RBP), whereas in the cerebrospinal fluid (CSF) TTR is the primary transporter of T4 [8,9]. TTR is also one of 30 human proteins associated with systemic amyloidoses, a group of disorders originally defined pathologically by the formation and aggregation of misfolded proteins which result in extracellular congophilic deposits that impair organ function [10]. Amyloidotic deposition of wild-type TTR occurs in the heart of 10–25% of humans older than 80 years, resulting in senile systemic amyloidosis (SSA), often leading to congestive heart failure [11,12]. TTR fibrillogenesis is accelerated by the presence of any of the approximately 100 different amyloidogenic mutations responsible for early-onset TTR amyloidoses (http://www.amyloidosismutations.com/mut-attr.php). These mutations are responsible for the reduced thermodynamic and/or kinetic stability of native tetrameric TTR [13], leading to the autosomal dominant disorders familial amyloid neuropathy (FAP), familial amyloid cardiomyopathy (FAC) and the rare leptomeningeal amyloidosis [14,15].

Abbreviations: AD, Alzheimer's disease; Aβ, amyloid-beta peptide; BSA, bovine serum albumin; CSF, cerebrospinal fluid; CM-H_2DCFDA, 2′,7′-dichlorodihydrofluorescein diacetate; DMSO, dimethylsulfoxide; DTT, dithiothreitol; D-PBS, Dulbecco's phosphate-buffered saline; ED, embryonic day; FAC, familial amyloid cardiomyopathy; FBS, fetal bovine serum; MTT, 3-(4,5-dimethylthiazol-2-yl)-2,5-diphenyltetrazolium bromide; NBM, neurobasal medium; HypF-N, N-terminal domain of the HypF protein from *Escherichia coli*; PMSF, phenylmethylsulfonyl fluoride; PSD-95, postsynaptic density protein 95; SDS-PAGE, sodium dodecylsulfate polyacrylamide gel electrophoresis; RBP, retinol binding protein charged with retinol; SSA, senile systemic amyloidosis; ThT, thioflavin T; T4, thyroxine; TTR, transthyretin

* Corresponding author. Tel.: +39 055 275 1222; fax: +39 055 7830303.
E-mail address: cristina.cecchi@unifi.it (C. Cecchi).

0925-4439/$ – see front matter © 2013 Elsevier B.V. All rights reserved.
http://dx.doi.org/10.1016/j.bbadis.2013.09.011

In spite of its link to human pathology, an anti-amyloidogenic effect that prevents fibril formation of the amyloid β (Aβ) peptide associated with Alzheimer's disease (AD) has been proposed for TTR. In 1993 it was found that in vitro amyloid fibril formation by $Aβ_{40}$ was inhibited by human CSF [16]. Although clusterin and apolipoprotein E were also present in the CSF, the responsible protein was later found to be TTR, through the formation of stable complexes between $Aβ_{40}$ and TTR [17]. In the same study it was also found that purified human TTR inhibited $Aβ_{28}$ fibril formation in vitro. Overexpression of human TTR in transgenic *Caenorhabditis elegans* expressing human $Aβ_{42}$ led to the reduction of ThS-positive Aβ deposits in the muscle cells of the nematodes [18]. Similarly, overexpression of WT human TTR in transgenic AD model mice carrying a mutant of the human Aβ gene led to a reduction in the Aβ deposits in the brains of these mice, while silencing the endogenous murine TTR genes accelerated disease progression in some mouse models [19,20]. Importantly, the reduction of amyloid deposition by overexpression of human TTR prevented the loss of spatial memory and learning usually seen in the AD mice [20].

Analyses of the in vitro interaction between human TTR and Aβ, using predominantly solid phase assay systems, have shown that TTR binds to all forms of Aβ: monomers, oligomers and fibrils [20–23]. The binding is highly dependent on the quaternary structure of TTR, with monomeric TTR binding Aβ with higher affinity than tetrameric TTR [23]. Moreover, the binding occurs with higher affinity for Aβ oligomers, aggregates and fibrils with respect to Aβ monomers [20,21,23,24]. In addition to inhibiting Aβ fibril formation, TTR was also shown to bind to preformed Aβ oligomers and fibrils and reduce their toxicity to murine primary neurons and human neuroblastoma SH-SY5Y cells [25].

In the light of the results obtained so far, one can hypothesize that TTR may act as an endogenous detoxifier of protein oligomers with potential pathological effects, in addition to inhibiting amyloid fibril formation [9]. However, it is not clear if such an effect is specific for Aβ oligomers or more generic, interacting with a variety of misfolded protein oligomers. In addition, previous data do not offer any insight into the mechanism by which TTR inhibits oligomer toxicity and on the TTR form responsible for such an effect. We have previously shown that the in vitro cytotoxicity of protein oligomers formed by Aβ, IAPP and HypF-N can be suppressed by molecular chaperones, with three of the five tested chaperones being extracellular [26]. In particular, it was shown that the chaperones inhibit the toxicity of the oligomers by binding to them and promoting their clustering into large aggregates, in the absence of any disaggregation or structural reorganization within the individual oligomers.

In this study we have examined the ability of three types of TTR having different tetramer stability, i.e., human TTR (hTTR), mouse TTR (muTTR) and an engineered monomer of human TTR carrying the F87M and L110M mutations (making it unable to form tetramers under our experimental conditions) (M-TTR), to suppress the in vitro toxicity of oligomers formed by two different peptides/proteins, i.e., $Aβ_{42}$ and HypF-N. muTTR is the most stable homotetramer that does not dissociate into partially unfolded monomers under physiologic conditions on any timescale [8]; hTTR forms stable tetramers but dissociates to monomers at a finite rate depending on environmental conditions [27], whereas M-TTR exists as a stable monomer [23,28,29]. As recently shown in experiments using these three conformers as well as a series of mutant human TTR tetramers of varying stability, the capacity of TTR to inhibit Aβ fibril formation is generally inversely related to tetramer stability [Li et al., submitted]. We now show that the three types of TTR display different protective effects against oligomer-induced cytotoxicity. We have gained molecular insight into the underlying mechanism by which suppression of oligomer cytotoxicity occurs in vitro, showing that the degree of TTR-mediated protection is greatest for the monomeric M-TTR and least for the most stable murine tetramer. Binding to the HypF-N and $Aβ_{42}$ oligomers appears to promote their clustering into larger aggregates in the absence of any structural reorganization.

2. Materials and methods

2.1. Materials

All reagents were of analytical grade or of the highest purity available. $Aβ_{42}$, bovine serum albumin (BSA), fetal bovine serum (FBS), hen egg white lysozyme (HEWL), pluronic acid F-127, staurosporine and other chemicals were from Sigma-Aldrich (Milan, Italy), unless otherwise stated. Fluo3-AM, calcein-AM and CM-H_2DCFDA (Life Technologies, CA, USA) were prepared as stock solutions in dimethylsulfoxide (DMSO), dried under nitrogen and stored in light-protected vessels at −20 °C until use. Neurobasal medium and B-27 were from Gibco (Life Technologies, CA, USA).

2.2. Cell cultures

Human SH-SY5Y neuroblastoma cells (ATCC Microbiology, Manassas, VA) were cultured in DMEM, F-12 Ham with 25 mM HEPES and $NaHCO_3$ (1:1) and supplemented with 10% FBS, 1.0 mM glutamine and antibiotics. Cell cultures were maintained in a 5.0% CO_2 humidified atmosphere at 37 °C and grown until they reached 80% confluence for a maximum of 20 passages.

2.3. Formation of protein oligomers

HypF-N was expressed, purified, and converted into toxic aggregates as previously reported [30]. $Aβ_{42}$ oligomers were produced as reported [31] and resuspended in the cell culture medium at a concentration of 12 μM. HypF-N oligomers were centrifuged at 16,100 rcf for 10 min, dried under N_2 and resuspended in cell culture media in the absence of cells (for cell biology tests) or in 20 mM potassium phosphate buffer at pH 7.0 (for biophysical/biochemical analysis). As reported, no significant dissolution of the HypF-N oligomers or change in morphology/structure could be detected after this procedure [30]. Native proteins were diluted to a final concentration of 12 μM into the same media. Oligomers were then incubated in the appropriate media for 1 h at 37 °C while shaking, in the absence or presence of each TTR, and then added to cultured cells or subjected to biophysical/biochemical analysis. The protein:TTR molar ratio was 10:1, unless stated otherwise (hTTR, muTTR and M-TTR are considered as tetramers).

2.4. Preparation of TTRs

hTTR, muTTR and M-TTR were prepared and purified in an *Escherichia coli* expression system as described elsewhere [28,32,33]. The three protein variants were purified by gel filtration on a Superdex 75 column (Amersham Biosciences, Inc.) in 10 mM phosphate buffer, 100 mM KCl, 1 mM EDTA pH 7.6 before each experiment to ensure that no aggregates were present in the starting material. Liquid chromatography–electrospray ionization mass spectrometry was used to confirm the molecular weight of the proteins.

2.5. MTT reduction assay

The effect of protein oligomers on cell viability was assessed using SH-SY5Y cells and primary neurons from rat brains seeded in 96-well plates, and using the 3-(4,5-dimethylthiazol-2-yl)-2,5-diphenyltetrazolium bromide (MTT) assay as described [34]. Preformed oligomers of HypF-N and $Aβ_{42}$ (12 μM monomer concentration) were incubated for 1 h in the absence or presence of hTTR, muTTR, M-TTR, haptoglobin, $α_2$-macroglobulin, HEWL or BSA (protein:TTR molar ratio was 10:1 unless otherwise stated; protein:haptoglobin, protein:HEWL and protein:BSA molar ratio was 5:1; protein:$α_2$-macroglobulin was 100:1), and then added to the cells. Each TTR (1.2 μM tetramer concentration) or 12 μM native HypF-N and $Aβ_{42}$ were also used as controls. In additional experiments, 1 μM staurosporine

(Sigma-Aldrich, Milan, Italy) was incubated for 1 h in cell culture medium in the absence or presence of each TTR and it was then added to the cells.

2.6. Measurement of intracellular Ca^{2+}

Preformed HypF-N and $A\beta_{42}$ oligomers (12 μM monomer concentration) were incubated for 60 min in the absence or presence of hTTR, muTTR or M-TTR (TTR concentration as described above), and then added to SH-SY5Y cells and rat hippocampal and cortical neurons seeded on glass coverslips for 60 min at 37 °C. Cells were also treated with 12 μM native HypF-N and $A\beta_{42}$ or each TTR at a tetramer concentration of 1.2 μM. To detect intracellular Ca^{2+} cells were then loaded with 10 μM fluo3-AM (Life Technologies, CA, USA) as described previously [35]. Cell fluorescence was analyzed by confocal Leica TCS SP5 scanning microscope (Mannheim, Germany) equipped with an argon laser source for fluorescence measurements at 488 nm and a Leica Plan Apo 63 × oil immersion objective. A series of optical sections (1024 × 1024 pixels) 1.0 μm in thickness was taken through the cell depth for each examined sample. The confocal microscope was set at optimal acquisition conditions, e.g., pinhole diameters, detector gain and laser powers. Settings were maintained constant for each analysis.

2.7. Caspase-3 activity

Preformed HypF-N and $A\beta_{42}$ oligomers (12 μM monomer concentration) were incubated for 1 h in the absence or presence of each TTR (TTR concentration as described above), and then they were added for 24 h to SH-SY5Y cells seeded on glass cover slips at 37 °C. Caspase-3 activity was evaluated by loading cells with FAMFLICA™ Caspases 3 & 7 solution [Caspase 3 & 7 FLICA kit (FAM-DEVDFMK), Immunochemistry Technologies, LLC, Bloomington, MN, USA], after treatment with oligomers. Cells were also treated with 12 μM native HypF-N and $A\beta_{42}$ or each TTR at a tetramer concentration of 1.2 μM. The analysis of cell fluorescence and the microscope settings was described above.

2.8. Thioflavin T assay

Preformed HypF-N oligomers (12 μM monomer concentration) were incubated for 1 h at 37 °C with shaking in the presence or absence of each TTR (HypF-N:TTR molar ratio as described above). Aliquots of these samples were added to a solution of 25 μM thioflavin T (ThT) dissolved in 25 mM phosphate buffer at pH 6.0, in order to obtain a 3.7-fold molar excess of dye. Final protein concentration was 6 μM. The steady-state intensity of fluorescence emission at 485 nm (excitation at 440 nm) was recorded at 37 °C. Each TTR (1.2 μM tetramer concentration) and 12 μM native HypF-N were also used as controls.

2.9. Pyrene fluorescence emission spectra

HypF-N variants carrying a single cysteine residue were labeled with N-(1-pyrene)maleimide and converted into toxic aggregates as previously reported [31] and then 4-fold diluted into 20 mM potassium phosphate buffer at pH 7.0. Fluorescence emission spectra of these samples were measured after 1 h of incubation at 37 °C under shaking in the absence and presence of each TTR. The spectra were acquired with 12 μM HypF-N, at 37 °C, with an excitation of 344 nm using a Perkin-Elmer LS 55 spectrofluorimeter (Wellesley, MA) equipped with a thermostated cell holder attached to a Haake F8 water bath (Karlsruhe, Germany), and a 1.5 × 1.5 mm quartz cell. The spectra were normalized to the intensity of the peak centered at 375 nm.

2.10. Intrinsic fluorescence

HypF-N oligomers and each TTR incubated in isolation and in combination as described before were centrifuged for 10 min at 16,100 rcf. The intrinsic fluorescence of the supernatants (SNs) were measured at 37 °C with excitation at 280 nm using a Perkin-Elmer LS 55 spectrofluorimeter (Wellesley, MA) equipped with a thermostated cell holder attached to a Haake F8 water bath (Karlsruhe, Germany), and a 2 × 10 mm quartz cell. The spectrum of HypF-N oligomers has been subtracted from that of TTR + HypF-N oligomers.

2.11. SDS-Page

HypF-N oligomers and each TTR incubated in isolation and in combination as described above were centrifuged for 10 min at 16,100 rcf. Pellets and SN aliquots were collected and mixed with 4× sample buffer with 20% 2-mercaptoethanol. Sodium dodecylsulfate polyacrylamide gel electrophoresis (SDS-PAGE) analysis was performed in accordance with Laemmli [36] using a 16% polyacrylamide gels. Proteins were visualized by Coomassie Blue staining (0.1% Coomassie Blue, 10% acetic acid, 40% methanol). The densitometric analysis was obtained using ImageJ software (NIH, Bethesda, MD, USA).

2.12. Atomic force microscopy

HypF-N/$A\beta_{42}$ oligomers (12 μM monomer concentration) were incubated for 1 h at 37 °C under shaking in 20 mM potassium phosphate buffer at pH 7.0, in the presence or absence of each TTR. Samples were diluted 1000-fold and immediately deposited on a freshly cleaved mica substrate and dried under a gentle nitrogen flux. Non-contact AC mode atomic force microscopy (AFM) images were acquired in air using a PicoSPM microscope equipped with an AC-mode controller (Molecular Imaging, Phoenix, AZ). Rectangular non-contact cantilever (model NSG01, NT-MDT Moscow, Russia), with typical resonance frequency of 150 kHz, were used. Oligomer sizes were measured from the height in cross section of the topographic AFM images.

2.13. Light scattering measurements

HypF-N oligomers (12 μM monomer concentration) were incubated for 1 h at 37 °C under shaking in 20 mM potassium phosphate buffer at pH 7.0 in the absence or presence of each TTR. Samples containing TTRs were also used as controls and filtered using 20 nm Anotop filters (Sigma-Aldrich, Milan, Italy). The measurements were performed using a Zetasizer Nano S DLS device from Malvern Instruments (Malvern, Worcestershire, UK), thermostated with a Peltier system and using a low-volume (45 μl), ultramicro cell (code 105.251-QS) from Hellma Analytics (Müllheim, Germany). Size distributions by intensity and total light-scattering intensity were determined at regular time-intervals over a period of 10 min. The temperature was maintained at 37 °C and the parameters were set manually on the instrument to allow the same settings in the various distributions acquired at different time-values. These included ten acquisitions each of 10 second duration, with cell position 4.2 cm and attenuator index 7. The reported data are the average of three consecutive measurements.

2.14. Turbidimetry

HypF-N oligomers (12 μM monomer concentration) were incubated for 1 h at 37 °C under shaking in 20 mM potassium phosphate buffer at pH 7.0 in the absence or presence of each TTR. Samples containing TTRs were also used as controls. Subsequently, the absorbance of the samples at 500 nm was measured using a Jasco V-630 UV–Vis Spectrophotometer (Tokyo, Japan) and a cell path of 0.1 cm. All the measurements were blank-subtracted.

2.15. Confocal microscopy analysis for TTR-HypF-N oligomer binding

HypF-N oligomers (at a corresponding monomer concentration of 48 μM) were incubated for different time lengths (0, 5, 15, 30

and 60 min) in the absence or presence of TTRs and then centrifuged to obtain pellet that were resuspended and incubated subsequently for 30 min at 37 °C in solutions containing: (i) 1:4000 rabbit polyclonal anti-HypF-N antibodies (Primm) and mouse monoclonal anti-TTR antibodies (Santa Cruz Biotechnology), (ii) 1:1000 Alexa Fluor 488-conjugated anti-rabbit secondary antibodies (Life Technologies, CA, USA), and (iii) Alexa Fluor 594-conjugated anti-mouse secondary antibodies (Life Technologies, CA, USA). After every incubation, samples were centrifuged for 10 min at 16,100 ×*g*, washed in PBS, and centrifuged again. Finally, the pellet was re-suspended in 20 μl PBS and spotted on glass coverslips. The cross-reactivity of oligomers was tested by subsequent incubations with primary and secondary anti-TTR antibodies. Confocal microscope images were acquired as described above.

2.16. Statistical analysis

Data was expressed as mean ± standard deviation (SD). Light scattering data was expressed as mean ± standard error of the mean (SEM). Comparisons between different groups were performed using ANOVA followed by Bonferroni's post-comparison test. A p-value lower than 0.05 was considered statistically significant.

3. Results

3.1. TTRs prevent oligomer-induced cytotoxicity in SH-SY5Y cells

We incubated oligomers formed from HypF-N and $A\beta_{42}$ in cell culture medium in the absence or presence of hTTR, muTTR or M-TTR for 1 h, then added the resulting mixtures to SH-SY5Y cells and measured the resulting cell viability using the MTT reduction assay. The two types of oligomers were toxic (Fig. 1A, B), as previously demonstrated [26]. The cells treated with oligomers preincubated with hTTR and M-TTR displayed no toxic effect showing MTT reduction similar to that of untreated cells, to cells treated with the native proteins or to cells treated with oligomers preincubated with haptoglobin or α_2-macroglobulin, two well known extracellular chaperones used here as positive controls for inhibition of oligomer toxicity (Fig. 1A, B). Conversely, muTTR shows a small insignificant protective effect (Fig. 1A, B). In addition, when the two oligomer types were incubated in the cell culture medium for 1 h with proteins that are not expected to possess chaperone properties, such as hen egg white lysozyme (HEWL) or bovine serum albumin (BSA), the oligomers maintained their toxicity (Fig. 1A, B). In these studies we did not examine the effect of the various TTRs on $A\beta_{42}$ and HypF-N oligomer formation.

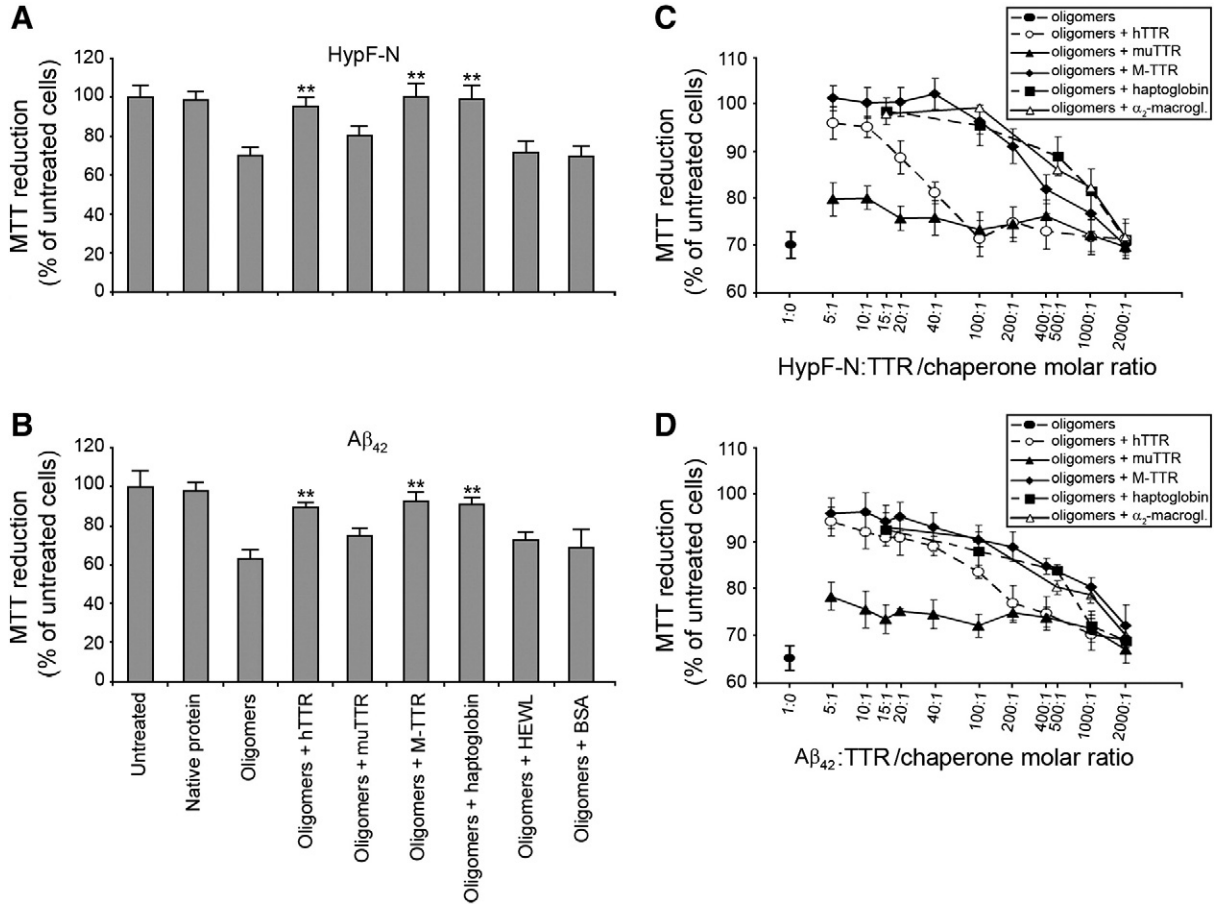

Fig. 1. Suppression of protein oligomer toxicity by TTRs. Preformed oligomers of HypF-N (A) and $A\beta_{42}$ (B) were resuspended in the cell culture medium, incubated for 1 h at a corresponding monomer concentration of 12 μM in the absence or presence of the indicated TTRs (protein:TTR molar ratio was 10:1), human haptoglobin (protein:haptoglobin molar ratio was 15:1), human α_2-macroglobulin (protein:α_2-macroglobulin molar ratio was 100:1), HEWL (protein:HEWL molar ratio was 5:1), or BSA (protein:BSA molar ratio was 5:1) and then added to SH-SY5Y cells. (C–D) Dose-dependent suppression of HypF-N (C) and $A\beta_{42}$ (D) oligomer toxicity by TTRs. Preformed oligomers of HypF-N and $A\beta_{42}$ were resuspended in the cell culture medium, incubated for 1 h in the absence (●) or presence of the indicated HypF-N:TTR/chaperone (C) and $A\beta_{42}$:TTR/chaperone (D) molar ratios and then added to SH-SY5Y cells. TTRs were always considered as tetramers in all HypF-N/$A\beta_{42}$:TTR molar ratio values. The scale on the *x* axis is logarithmic. Cell viability was expressed as percent of MTT reduction in treated cells with respect to untreated cells (taken as 100%). The values shown are means ± SD of three independent experiments carried out in quadruplicate. The single, double and triple asterisks indicate a significant difference ($p \leq 0.05$, $p \leq 0.01$, $p \leq 0.001$, respectively) relative to the experiment with oligomers only.

We repeated the experiments described above for HypF-N and $A\beta_{42}$ oligomers by varying the concentration of each TTR in the 1 h pre-incubation solution, while maintaining a constant concentration of HypF-N and $A\beta_{42}$. M-TTR was found to suppress the toxicity of HypF-N and $A\beta_{42}$ oligomers even at low concentration with an efficacy similar to haptoglobin and α_2-macroglobulin (Fig. 1C, D). M-TTR remained effective even at an HypF-N:TTR and $A\beta_{42}$:TTR molar ratio of 400:1, becoming ineffective at a molar ratio of 1000:1 both for HypF-N and $A\beta_{42}$ (Fig. 1C, D). hTTR is also effective, but at higher concentrations; indeed, hTTR inhibited toxicity until a HypF-N:TTR and $A\beta_{42}$:TTR molar ratio of 40:1 and 100:1, respectively, only becoming ineffective at molar ratios of 100:1 for HypF-N and 200:1 for $A\beta_{42}$. muTTR did not show any protective effect, even at low molar ratios (Fig. 1C, D).

We also evaluated the intrinsic cytotoxic effect of each TTR variant in the absence of the oligomers. Our results showed that under our experimental condition (preincubation for 1 h at 37 °C) M-TTR significantly decreased the MTT reduction of the SH-SY5Y cells by ca. 20% (Suppl. Fig. 1A); conversely, hTTR and muTTR did not show significant toxic effects (Suppl. Fig. 1A), whereas it has been demonstrated that hTTR is cytotoxic if produced or exposed to cold temperature [37,38]. These results indicate that M-TTR alone is toxic to cells, as previously demonstrated [39], whereas preincubation of M-TTR with toxic HypF-N and $A\beta_{42}$ oligomers suppresses both toxic effects, suggesting an interaction between oligomers and monomeric TTR with mutual suppression of toxicity.

To assess whether the three types of TTR can protect the cells from other forms of stress, or if they are specific for protein oligomers, we incubated the cells with staurosporine, a well-known apoptosis inducer. We found that a concentration of 1 μM of staurosporine decreased the MTT reduction of the cells to a level similar to that of preformed protein oligomers under our conditions. The staurosporine toxicity was not reduced by any of the three TTRs (Suppl. Fig. 1B).

These results indicate that hTTR and M-TTR can suppress or markedly decrease the toxicity of oligomers formed by two different peptides and proteins. The suppression is specific for TTRs or chaperones (relative to other proteins) with respect to toxicity induced by preformed protein oligomers (not other forms of stress).

3.2. TTRs inhibit oligomer-mediated intracellular Ca^{2+} influx, ROS production and membrane permeabilization

The influx of Ca^{2+} ions from the extracellular space into the cytosol across the cell membrane has been recognized to be an early biochemical change undergone by cells exposed to deleterious protein oligomers including HypF-N and $A\beta_{42}$ oligomers [35,40–44]. Here we compared the ability of the different types of TTR to inhibit the influx of Ca^{2+} caused by soluble oligomers of HypF-N and $A\beta_{42}$ after their preincubation for 1 h in the cell culture medium before addition to the SH-SY5Y cells. Both HypF-N and $A\beta_{42}$ oligomers induced a sharp increase in cytosolic free Ca^{2+} levels (Fig. 2). Preincubation with hTTR and M-TTR was found to inhibit the increase of intracellular Ca^{2+} levels caused by the oligomers, whereas muTTR showed a lower protective effect (Fig. 2). In addition, the degree of Ca^{2+}-derived fluorescence was found to decrease exponentially with the time of preincubation with M-TTR and hTTR (Suppl. Fig. 2); in particular, M-TTR prevented the Ca^{2+} spike after only 15 min of preincubation (Suppl. Fig. 2).

Similar results were obtained from analyzing intracellular ROS production and membrane permeability. HypF-N oligomers induced a sharp increase in ROS levels in our cell model (Suppl. Fig. 3A). hTTR and M-TTR inhibited the increase of intracellular ROS levels caused by the oligomers, with the degree of ROS-derived fluorescence decreasing exponentially with the time of preincubation (Suppl. Fig. 3A); M-TTR prevented the ROS production after only 15 min of preincubation (Suppl. Fig. 3A). In contrast, mTTR did not show any protective effect (Suppl. Fig. 3A).

Confocal microscopy analysis of SH-SY5Y cells pre-loaded with calcein-AM showed that cell exposure to HypF-N toxic oligomers resulted in a significant decrease of fluorescence intensity in our cells, indicating increased membrane permeabilization (Suppl. Fig. 3B). In contrast, the reduction in calcein fluorescence was prevented when the cells were treated with oligomers preincubated with hTTR and M-TTR, with the degree of calcein-derived fluorescence increasing exponentially with the time of preincubation (Suppl. Fig. 3B). In particular, the reduction of permeabilization occurred even more quickly in the presence of M-TTR. mTTR did not show any protective effect (Suppl. Fig. 3B).

3.3. TTRs prevent oligomer-induced apoptosis

We then evaluated whether the different capacities of TTRs to protect cytosolic Ca^{2+} influx, ROS production and membrane permeabilization induced by HypF-N and $A\beta_{42}$ oligomers also resulted in different abilities to prevent cell death. We measured Caspase-3 activity, a well recognized apoptotic marker, using confocal microscopy (Fig. 3) [45]. Fluorescence microscopy images and the corresponding semi-quantitative values of the green fluorescence signal show that hTTR and M-TTR significantly prevented the apoptotic response induced by HypF-N and $A\beta_{42}$ oligomers (Fig. 3A, B; $p < 0.01$). muTTR also showed a significant protection but it was less marked than that of the other TTRs (Fig. 3A, B; $p < 0.05$). A similar trend was observed in analyzing chromatin condensation by using the Hoechst 33342 dye, a fluorescent marker that binds to the highly condensed chromatin present in the nuclei of apoptotic cells [46] (Suppl. Fig. 4).

3.4. TTRs prevent oligomer-induced toxicity and inhibit colocalization of HypF-N aggregates with PSD-95 in rat primary neurons

We assessed the relative protective capacity of the three different TTRs for rat hippocampal and cortical neurons using the MTT reduction assay. The HypF-N oligomers were toxic to rat hippocampal and cortical neurons (Suppl. Fig. 5A,B). The neurons treated with HypF-N oligomers pre-incubated with hTTR and M-TTR were found to reduce MTT to levels similar to untreated cells and to cells treated with the native protein (Suppl. Fig. 5A, B); conversely, muTTR showed a small and non-significant protective effect (Suppl. Fig. 5A, B). We also evaluated the intrinsic cytotoxic effect of each TTR variant in the absence of the oligomers. M-TTR significantly decreased the MTT reduction of neurons by 25% (Suppl. Fig. 5A, B); conversely hTTR and muTTR did not show any significant toxic effect (Suppl. Fig. 5A, B). These results indicate that as previously shown for Aβ induced cytotoxity, hTTR and M-TTR are able to suppress HypF-N oligomer-induced toxic effects in both immortalized cell cultures and primary neurons.

To investigate the mechanism of action by which TTRs protect cultured primary neurons from toxic HypF-N oligomers, we examined the colocalization between oligomers and PSD-95 in cultured primary hippocampal neurons. It has previously been shown that binding sites of $A\beta_{42}$ and HypF-N oligomers on neurons overlap with PSD-95 [47–49]. A remarkable degree of colocalization was observed between HypF-N oligomers and PSD-95, whereas no colocalization was observed in untreated cells or in cells treated with native HypF-N (Suppl. Fig. 5C). Preincubation of HypF-N oligomers with hTTR or M-TTR for 1 h was found to inhibit oligomer binding to the cell membrane, thus preventing the colocalization with PSD-95 (Suppl. Fig. 5C). Preincubation of HypF-N oligomers with muTTR also decreased colocalization, but to a lower level than observed for the other TTRs (Suppl. Fig. 5C). In particular, the fraction of HypF-N puncta colocalizing with PSD-95 puncta was 21.4 ± 3.1% (n = 18) for oligomers preincubated with hTTR for 1 h, 35.7 ± 1.2% (n = 18) for oligomers preincubated with muTTR for 1 h and 16.5 ± 1.2% (n = 18) for oligomers preincubated with M-TTR for 1 h.

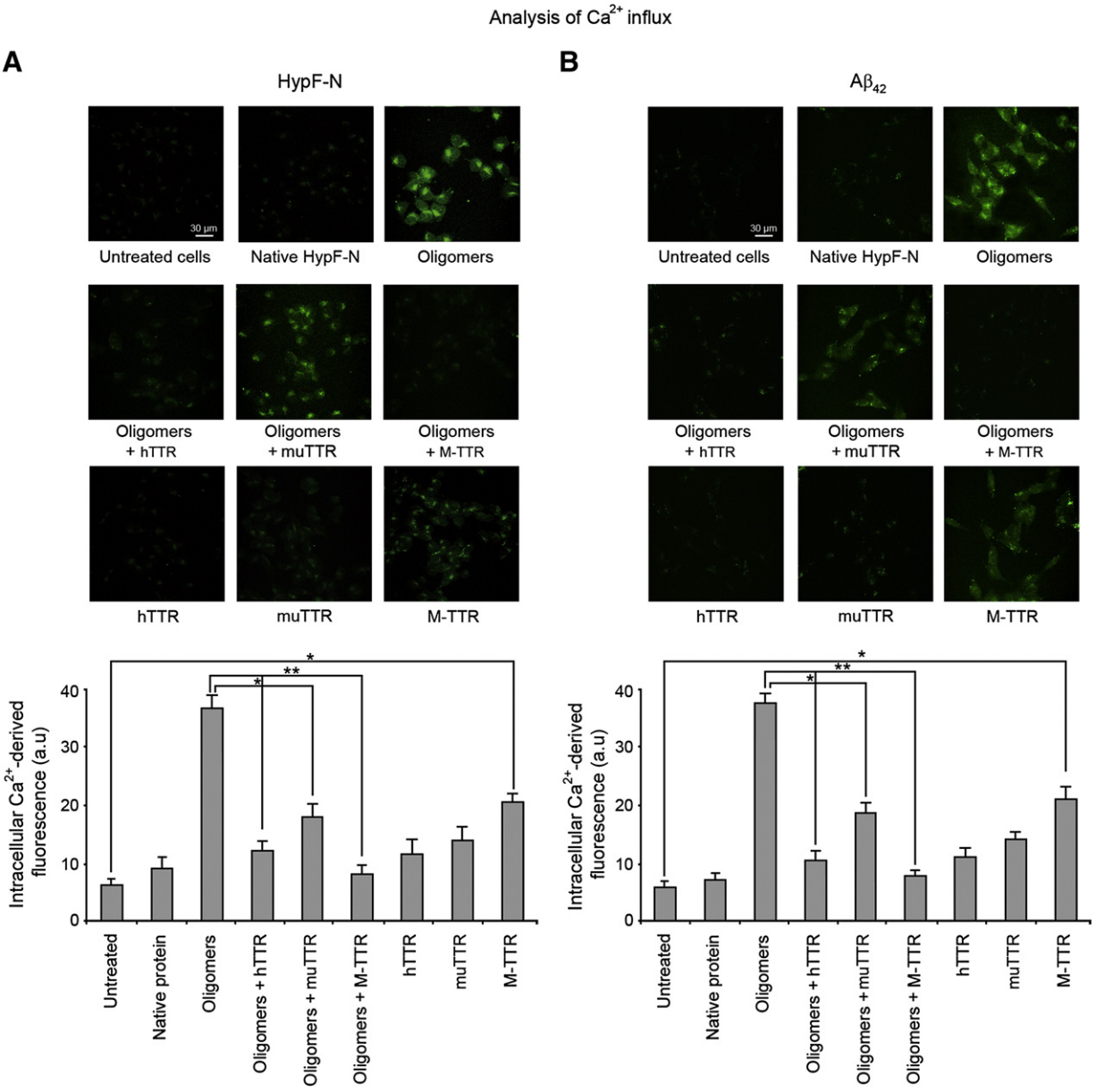

Fig. 2. Representative confocal scanning microscope images showing intracellular Ca^{2+} levels in SH-SY5Y cells. Preformed oligomers of HypF-N (A) and $A\beta_{42}$ (B) were resuspended in the cell culture medium, incubated for 1 h at a corresponding monomer concentration of 12 μM with or without the indicated TTRs (protein:TTR molar ratio was 10:1) and then added to SH-SY5Y cells for 1 h. The figure also shows untreated cells, cells exposed for 1 h to the native protein, to toxic oligomers (12 μM monomer) and to the indicated TTRs alone (1.2 μM tetramer or 4.8 μM monomer). The green fluorescence arises from the intracellular Fluo3 probe bound to Ca^{2+}. The corresponding semi-quantitative values of the green fluorescence signals are shown below each set of images. Statistics as in Fig. 1.

hTTR and M-TTR were also found to prevent the oligomer-mediated intracellular Ca^{2+} increase in both hippocampal (Suppl. Fig. 6A) and cortical neurons (Suppl. Fig. 6B). They also inhibited intracellular ROS production in hippocampal neurons (Suppl. Fig. 6C). These results show that preincubation of the HypF-N oligomers with hTTR and M-TTR, and to a lesser extent muTTR, inhibit the binding of the oligomers at PSD-95 containing sites and reduce the toxicity of the oligomers for neurons.

3.5. The molecular structure of HypF-N oligomers is preserved in the complexes with TTRs

In order to investigate the mechanism by which TTRs suppress the toxicity of protein oligomers, we have chosen to focus on the toxic oligomers of HypF-N. Indeed, under different experimental conditions, HypF-N can aggregate into toxic (type A, the same used in the present work) or nontoxic (type B) oligomers; using atomic force microscopy (AFM) the two species are morphologically similar (ca. 2–6 nm in height) and bind ThT to similar levels, making it possible to carry out valuable control experiments [30]. Thus, HypF-N oligomers appear to be highly stable, making them easy to handle in our experiments [30]. We have, however, carried out the key experiments also on $A\beta_{42}$ oligomers (see below).

To shed light on the behaviors of the various TTRs and on the molecular mechanism by which they exert their protection against HypF-N oligomers we investigated the oligomeric state and the molecular structure of HypF-N oligomers after preincubation with various TTRs. To assess whether the oligomers can be dissolved by the different types of TTR, we exploited the ability of the HypF-N oligomers, unlike native HypF-N, to bind to ThT and increase its fluorescence [30] (Fig. 4A).

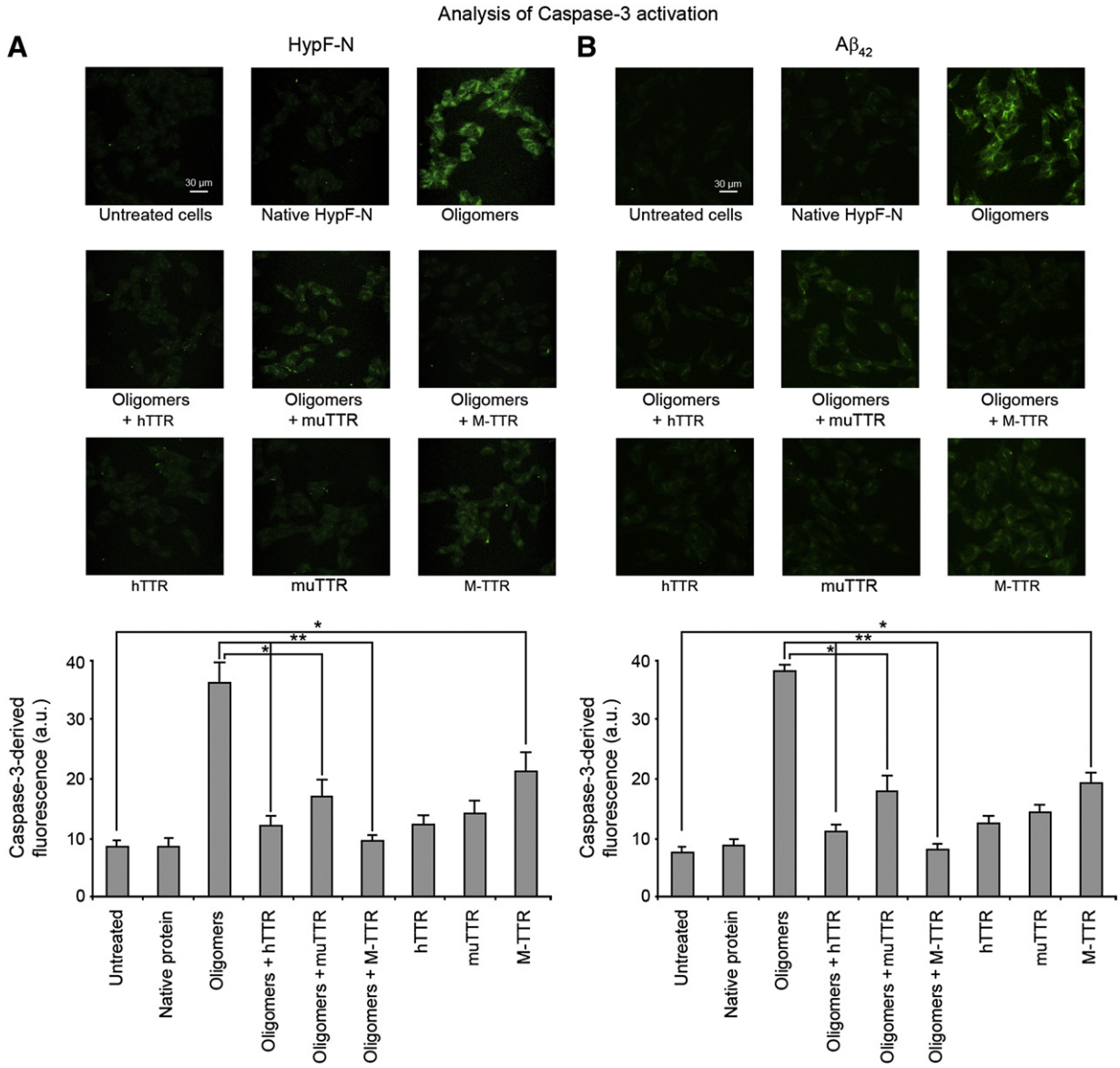

Fig. 3. Representative confocal microscope images showing Caspase-3 activation in SH-SY5Y cells. Preformed oligomers of HypF-N (A) and $A\beta_{42}$ (B) were resuspended in the cell culture medium, incubated at a corresponding monomer concentration of 12 μM with or without the indicated TTRs (protein:TTR molar ratio was 10:1) for 1 h and then added to SH-SY5Y cells for 24 h. The figure also shows untreated cells, cells exposed for 1 h to the native protein, to toxic oligomers (12 μM monomer) and to the indicated TTRs alone (1.2 μM tetramer or 4.8 μM monomer). Caspase-3 activity, assessed using the fluorescent probe FAM-FLICA™ Caspases 3 & 7, is indicated by green fluorescence. The corresponding semi-quantitative values of the green fluorescence signals are shown below each set of images. Statistics as in Fig. 1.

HypF-N oligomers incubated for 1 h in a phosphate buffer at neutral pH cause a seven to eight fold increase of ThT fluorescence, and the same increase was observed when the oligomers were preincubated in the same buffer for 1 h with each of the TTRs (Fig. 4A). To exclude the possibility that TTRs bind ThT, in parallel we also analyzed samples containing only TTRs under identical conditions and detected no increase of ThT fluorescence in these cases (Fig. 4A). Overall, these results show that HypF-N oligomers remain stable and do not undergo disaggregation after TTR treatment.

Subsequently, we asked whether the oligomers are structurally reorganized at the molecular level by the TTRs (Fig. 4B). Differences in the structure of toxic and non-toxic oligomers have been detected using the fluorescent probe pyrene, a structural probe for changes in oligomers exposed to chaperones [30]. We determined the degree of packing of the oligomers through the acquisition of fluorescence spectra of oligomers labeled with pyrene. This method consists in creating HypF-N variants containing a single cysteine at different positions along the sequence, label them with pyrene and allow the labeled mutants to aggregate. When two pyrene molecules are close to each other (within 10 Å of distance), excited state dimers called excimers form and can be detected as a peak at 440–470 nm [50–52]. It has been shown that toxic and non-toxic HypF-N oligomers can be distinguished by differences in their pyrene emission spectra [30].

Three variants of HypF-N containing a single cysteine residue at position 25, 55 or 87, all located in the major hydrophobic regions, were labeled with pyrene, allowed to aggregate and were transferred to phosphate buffer at neutral pH for 1 h with or without the different forms of TTR. The fluorescence spectra acquired for the oligomers in either the presence or absence of the TTRs were very similar with none showing an excimer band (Fig. 4B). Moreover, the ratio of the excimer-to-monomer fluorescence intensity (FI_{440nm}/FI_{375nm}) did not change following preincubation with any TTR, remaining lower in all cases than the

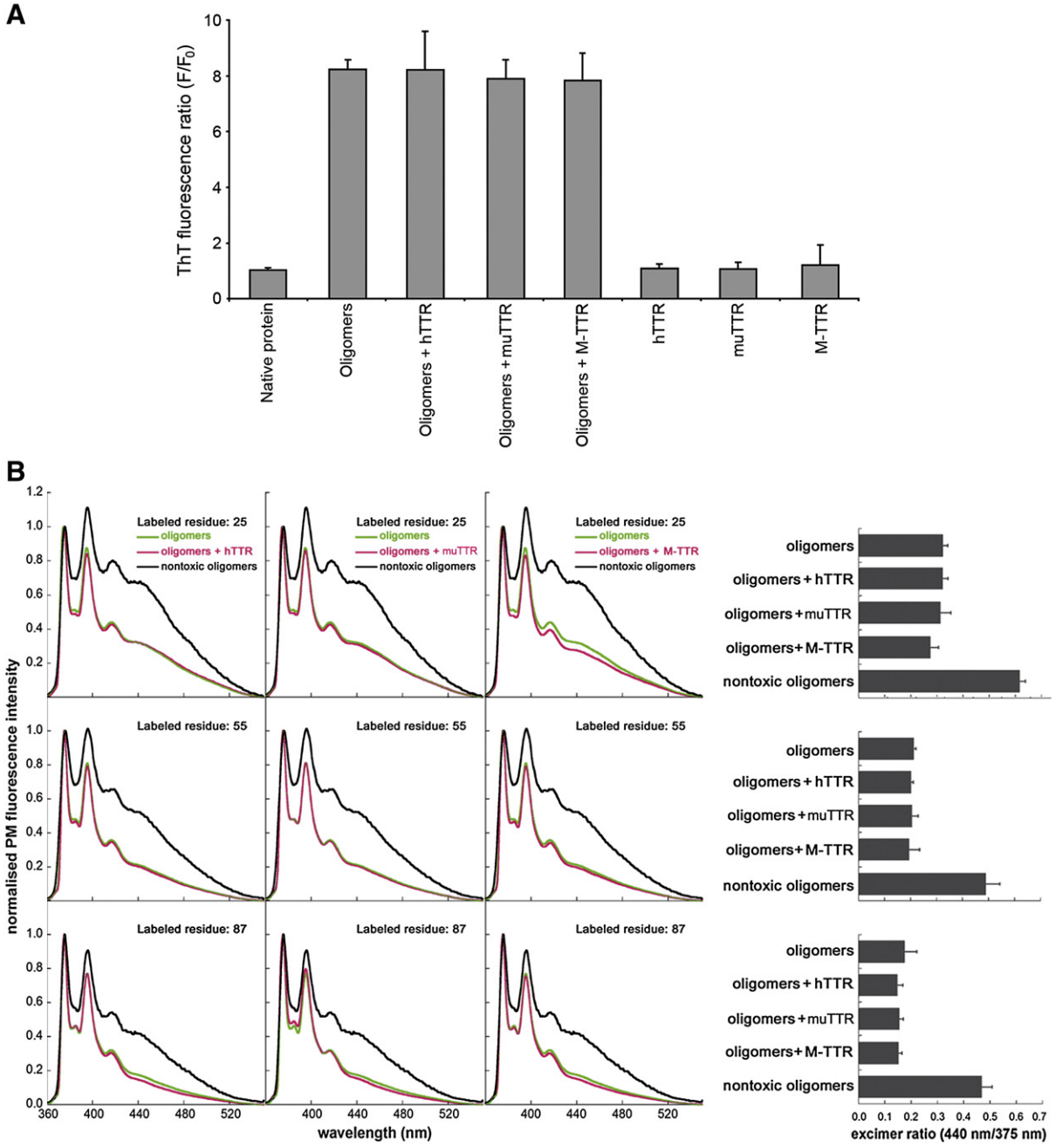

Fig. 4. TTRs do not dissolve and do not remodel HypF-N oligomers. (A) ThT fluorescence at 485 nm (excitation 440 nm) in the presence of the indicated protein components following preincubation for 1 h in 20 mM phosphate buffer at pH 7.0 in the absence or presence of different types of TTR. The ratio between the ThT fluorescence in the presence (F) and absence (F_0) of proteins is reported; data are means ± SD of three independent experiments. The HypF-N concentration was 48 μM (in monomer units) and the HypF-N:TTR molar ratio was 10:1. (B) Fluorescence emission spectra of samples containing HypF-N oligomers labeled with pyrene at positions 25 (top), 55 (middle) and 87 (bottom). The spectra were acquired at 12 μM HypF-N concentration following 1 h incubation in the absence (green) or presence (pink) of hTTR (left panels), muTTR (middle panels) or M-TTR (right panels). For comparison, the corresponding spectra of nontoxic oligomers are reported in each graph (black). The spectra have been normalized to the intensity of the peak centered at 375 nm. The molar ratio of HypF-N:TTR was 10:1. On the right, the excimer-to-monomer fluorescence intensity (Fl_{440nm}/Fl_{375nm}) of each sample and of the nontoxic oligomers [30] is reported.

corresponding value measured for the non-toxic oligomers (Fig. 4B). These results show that none of the TTRs promote structural re-organization of the toxic HypF-N oligomers.

3.6. TTRs bind to the oligomers

To determine whether TTRs bind to the oligomers we used TTR-derived intrinsic fluorescence and SDS-PAGE. HypF-N oligomers sediment at relatively low centrifugal force; therefore, if the TTRs bind to the oligomers and the interaction between them is stable, the concentration of the TTRs in the supernatant will decrease following centrifugation, depending on the strength of the interaction. HypF-N oligomers and TTRs were incubated for 1 h in phosphate buffer at pH 7.0 then centrifuged to separate the pellet fraction (P), which contains the TTR bound to the oligomers, from the supernatant (SN), which contains the soluble unbound TTR. The amount of TTR in the SN was measured by its intrinsic fluorescence (Fig. 5A–C). The fluorescence spectra of the SNs collected from the samples in which oligomers and hTTR or M-TTR were present were

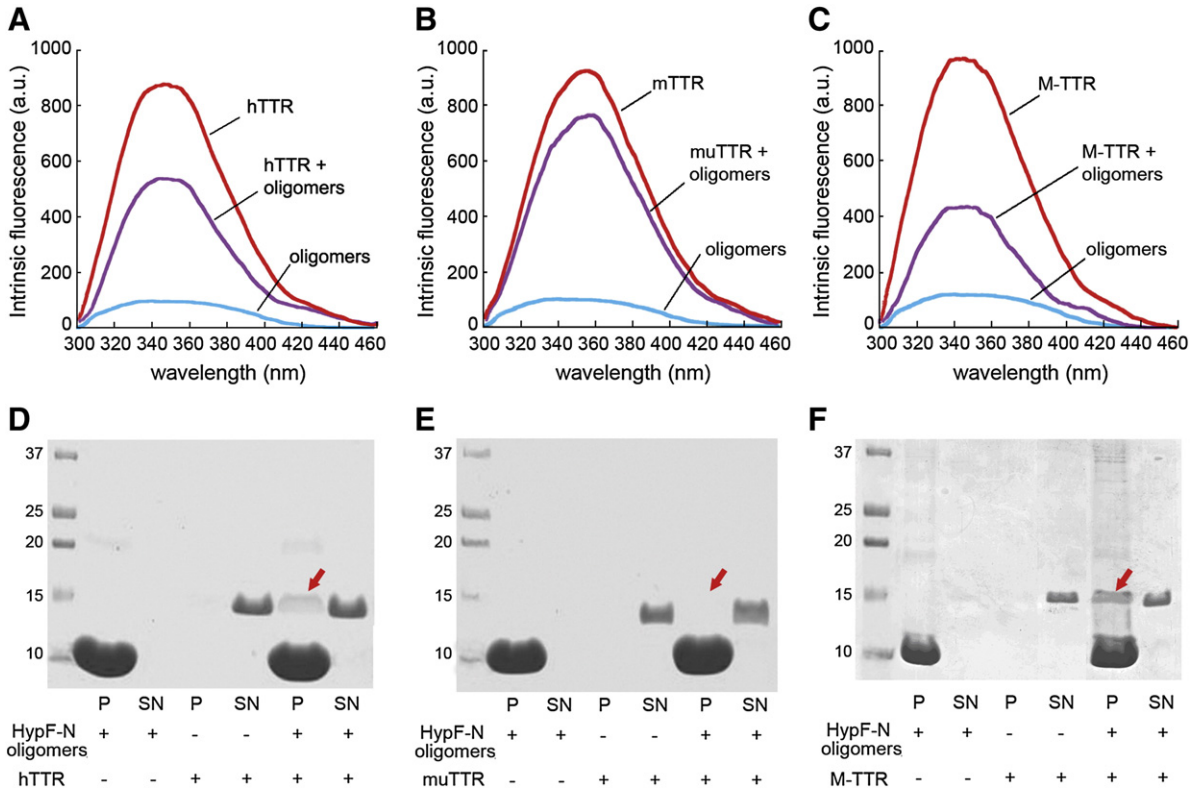

Fig. 5. TTRs interact with HypF-N oligomers. (A–C) Intrinsic fluorescence spectra of the SN fractions obtained after centrifugation of samples containing preformed HypF-N oligomers (blue), TTR (red) and HypF-N oligomers + TTR (purple). The fluorescence emission spectra (excitation at 280 nm) were acquired at 37 °C. The spectrum of HypF-N oligomers has been subtracted from that of TTR + HypF-N oligomers to eliminate its contribution. (D–F) SDS-PAGE analysis of the insoluble (P) and soluble (SN) fractions obtained from samples containing preformed HypF-N oligomers (lanes 2, 3), TTR (lanes 4, 5) and preformed oligomers treated for 1 h with TTR (lanes 6, 7). The HypF-N concentration was 48 μM (in monomer units) and the molar ratio of HypF-N:TTR was 10:1.

less intense than the corresponding ones in which only the TTRs were present, indicating that a fraction of hTTR, and to a greater extent M-TTR, is bound to the oligomers. In contrast, the fluorescence spectrum of the SN collected from the sample containing oligomers and muTTR was similar to that in which only muTTR was present.

As a further evidence of binding, the pellet and supernatant fractions collected in each experiment were analyzed by SDS-PAGE. In the samples containing oligomers or TTR alone, the HypF-N monomer (MW ~10.5 kDa) and the TTR monomer (MW ~14 kDa) were found only in the pellet and SN fractions, respectively (Fig. 5D–F). In the sample containing both HypF-N oligomers and M-TTR, the HypF-N band was present only in the pellet fraction, whereas M-TTR was found to partition between the pellet (49.8% ± 2.6) and SN fractions (Fig. 5F). This result confirms that a fraction of M-TTR is bound to the oligomers. Similar results, but with evidence of a smaller fraction bound in the pellet (24.1% ± 3.1), were obtained with hTTR (Fig. 5D). In contrast, we found muTTR only in the SN fraction, suggesting that muTTR did not bind to HypF-N oligomers under these conditions (Fig. 5E). These results suggest that the ability of TTRs to bind HypF-N oligomers correlates inversely with TTR tetramer stability.

3.7. TTRs promote the assembly of the oligomers into larger species

To investigate whether the binding of TTRs to the oligomers promotes their further assembly, we first used AFM. Discrete HypF-N oligomers with a height of 1–4 nm were observed by AFM in the absence of TTR (Fig. 6A), but significantly larger aggregates were evident after 1 h incubation in the presence of M-TTR and, to a lower extent, hTTR (Fig. 6A). More complex structures were observed in the presence of M-TTR, consisting of very large aggregates of irregular shape with typical heights of a few tens of nanometers. Large assemblies were not observed in samples containing oligomers with muTTR (Fig. 6A), or in samples containing only TTR. Similar results were obtained with $A\beta_{42}$ oligomers and TTRs (Suppl. Fig. 7A).

As additional evidence of the ability of TTRs to promote oligomer assembly, we took advantage of light scattering measurements. In the presence of M-TTR, and hTTR to a lower extent, light scattering intensity increased, indicating that the oligomers were larger in size (Fig. 6B). Accordingly, these results were confirmed with turbidimetry measurements at 500 nm, which revealed a similar trend, presumably related to the lower sensitivity of this method (Fig. 6C).

The AFM, light scattering and turbidity results show that M-TTR and hTTR promote the assembly of the HypF-N oligomers into larger species but do not provide information on whether or not the large HypF-N aggregates include the TTRs. The oligomers can also be observed with confocal microscopy because, unlike free TTRs, they readily adhere to the glass coverslips (Fig. 7). Images obtained using HypF-N oligomers incubated for 1 h with TTRs show larger aggregates, with M-TTR and hTTR colocalizing with the large oligomer clusters (Fig. 7). By contrast, images obtained using HypF-N oligomers and TTRs in the absence of 1 h incubation showed no large oligomers (Fig. 7). Indeed, incubation of HypF-N oligomers with M-TTR promoted formation of large aggregates in a time-dependent manner (Fig. 7, bottom panel). Interestingly, the TTRs appear within the structural core rather than on the surface of these larger aggregates, suggesting that they promote the formation of such large aggregates rather than binding and stabilizing them after they are formed (Fig. 7). On the other hand, mTTR did not colocalize with the oligomers. This technique also showed that the M-TTR and hTTR were bound only to the large clusters of oligomers, not to single oligomers, confirming that the binding promotes their further assembly into clusters. Similar results were obtained with $A\beta_{42}$ oligomers and M-TTR (Suppl. Fig. 7B).

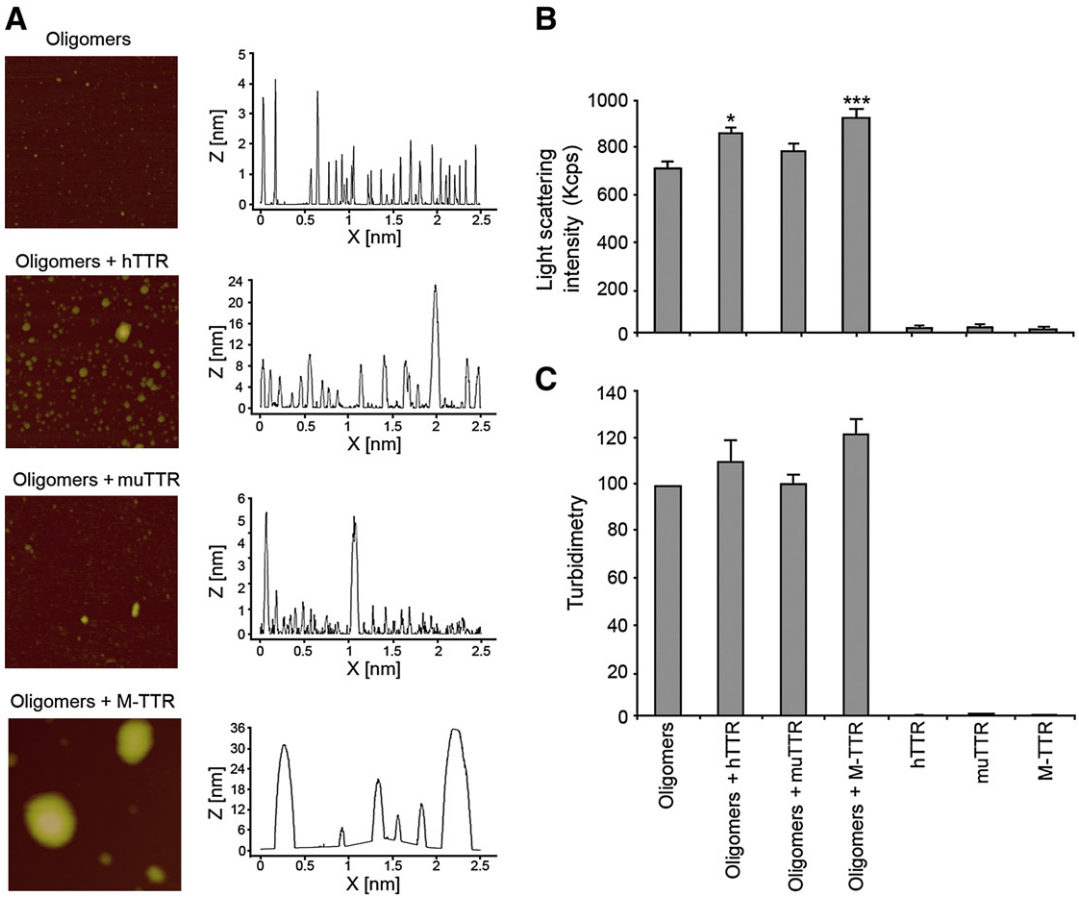

Fig. 6. Assembly of HypF-N oligomers induced by TTRs. (A) AFM images and corresponding height analysis of HypF-N oligomers preincubated with or without TTRs. Preformed oligomers of HypF-N were resuspended in phosphate buffer pH 7.0, incubated for 1 h at a corresponding monomer concentration of 48 μM in the absence or presence of the indicated TTRs (HypF-N:TTR molar ratio was 10:1) and then deposited on mica; the scan size is 1 μm. Z range: 5 nm (oligomers), 24 nm (oligomers + hTTR), 6 nm (oligomers + muTTR), 36 nm (oligomers + M-TTR). (B) Light scattering intensity measurements of HypF-N oligomers preincubated with or without TTRs and TTRs alone. The light scattering intensities were measured at 48 μM HypF-N and at a HypF-N:TTR molar ratio of 10:1. (C) Measurements of turbidimetry at 500 nm of HypF-N oligomers incubated with or without TTRs and TTRs alone. Conditions as in (B). The values shown are means ± SEM of five independent experiments. The single and the triple asterisks indicate significant difference ($p \leq 0.05$ and $p \leq 0.001$, respectively) relative to the experiment with oligomers only.

4. Discussion

TTR was shown to inhibit aggregation and amyloid plaque formation of Aβ both in vitro and in vivo [17–21, 23, Li et al., submitted]. Analyses carried out in vitro have shown that TTR binds monomeric Aβ, explaining its ability to prevent aggregation of the peptide [22, 23, Li et al., in preparation]. However, in experiments using various forms of Aβ fixed to solid surfaces (e.g., nitrocellulose membranes or Biacore chips) TTR-Aβ binding was found to occur with higher affinity for aggregated Aβ, such as oligomers and fibrils, relative to monomeric Aβ, with monomeric TTR exhibiting stronger binding than tetrameric TTR [20, 21, 23, Li et al., submitted]. The high affinity between monomeric TTR and aggregated Aβ suggests an important role for such an interaction in vitro. Indeed, TTR was shown to bind to preformed Aβ oligomers and reduce their toxicity to murine primary neurons and human neuroblastoma SH-SY5Y cells [25]. In those studies, the suppression of TTR-mediated toxicity was not due to the ability of TTR to inhibit Aβ aggregation, but appeared to act on preformed oligomers. Subsequent studies have shown that hTTR both inhibits Aβ oligomer formation and interacts with small Aβ oligomers to prevent the formation of nucleation competent seeds [Li et al., submitted].

Here, we found that TTR is able to suppress the toxicity of extracellularly added oligomers formed by two different peptides/proteins, namely $Aβ_{42}$ and HypF-N, adding new data to the preliminary observation obtained with $Aβ_{42}$ [25]. TTR was found to inhibit the influx of Ca^{2+} caused by the oligomers, thus eliminating the occurrence of later effects, manifested as oxidative stress, membrane leakage and apoptosis. In addition, the observed dependence of the degree of protection on the time of preincubation between oligomers and TTR indicates that TTR suppresses oligomer toxicity by interacting with the oligomers, rather than through a separate protective pathway mediated by direct interaction of TTR with the cells. Overall, therefore, these findings reveal that the deleterious effects produced by interaction of misfolded protein oligomers with cell membranes can be abolished by TTR.

The three types of TTR examined here, namely hTTR, muTTR and M-TTR, were found to display different protective effects against oligomer-induced cytotoxicity. Indeed, monomeric M-TTR was able to protect SH-SY5Y neuroblastoma cells and rat primary neurons against oligomer-induced cytotoxicity; the highly stable tetrameric muTTR only showed only a small non-significant protective effect, whereas the less stable tetrameric hTTR had an effect intermediate between the two forms, or displayed a protective action more slowly or at higher concentrations than M-TTR. Hence, the ability of TTR to protect neuronal cells and neurons against these misfolded protein oligomers in vitro correlates inversely with the stability of the tetramer.

To shed light on the molecular mechanism by which TTR prevents cytotoxicity, we focused on HypF-N oligomers, probing their oligomeric state and molecular structure after the incubation with TTRs in vitro. Using ThT fluorescence we found that TTR does not disaggregate the

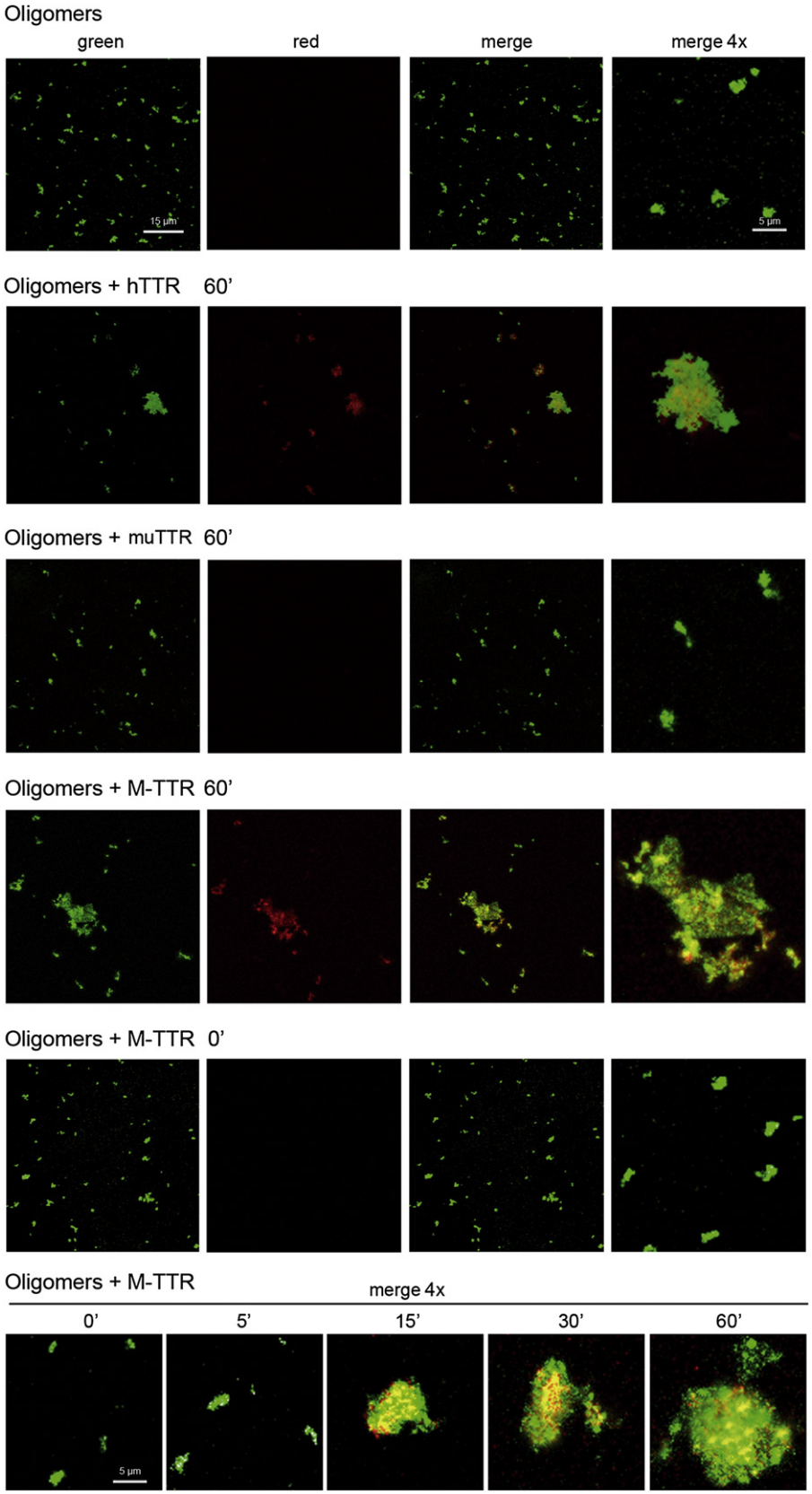

Fig. 7. Colocalization of HypF-N oligomers and TTRs. Representative confocal microscope images with HypF-N oligomers incubated for the indicated time lengths in the absence or presence of the indicated TTRs and treated with anti-HypF-N (green) and anti-TTR (red) antibodies. The colocalization of oligomers and TTRs is shown in the merged images (yellow dots). The HypF-N concentration was 48 μM (in monomer units) and the molar ratio of HypF-N:TTR was 10:1.

preformed oligomers. Nor does it appear to promote a structural reorganization of the discrete oligomers, as shown by site-directed pyrene labeling. Rather, TTR was found to bind to the oligomers, as determined with SDS-PAGE, intrinsic fluorescence and confocal scanning microscopy, and promote their further assembly into larger aggregates, as shown by AFM, light scattering measurements and turbidimetry. The ability of TTR to bind to the oligomers and cause their clustering was also found for $A\beta_{42}$ oligomers, using AFM and confocal scanning microscopy. Clearly, the ability of TTR to bind to and further assemble preformed HypF-N and $A\beta_{42}$ oligomers correlated again inversely with its stability, as the efficiency of such process followed the same order as that found for toxicity suppression, i.e., M-TTR > hTTR > mTTR. These data also suggest that the size of extracellular protein aggregates is an inverse correlate of their toxicity. The TTR-induced oligomer clusters are characterized by a reduction in their exposed hydrophobic surface and diffusional mobility, both of which are expected to reduce their toxicity to cells [26,53–56].

Recent structural analyses of the TTR/Aβ interaction have revealed a complex set of interactions with hTTR tetramers binding the Aβ monomer in the T4 binding pocket to inhibit Aβ aggregation and cytotoxicity [Li et al., submitted]. By contrast, M-TTR was found to interact preferentially with Aβ oligomers [Li et al., submitted], and this observation is consistent with the better binding of M-TTR to HypF-N oligomers shown here. Nevertheless, the M-TTR/Aβ oligomer interaction was not found to be associated with a size increase of the oligomers [Li et al., submitted], whereas in our experimental conditions the interaction between M-TTR and HypF-N/$A\beta_{42}$ oligomers was found to involve further clustering of the oligomers. The interaction showed by Li et al. was obtained under different conditions compared to those used in the present study. M-TTR was added to the aggregation assay where Aβ was initially monomeric [Li et al., submitted]. Here we added M-TTR to pre-formed HypF-N/$A\beta_{42}$ oligomers. Such a difference parallels the data showed by Ojha et al. showing that the chaperone HspB1 converted the preformed oligomers of Aβ into large aggregates, whereas, the incubation with Aβ monomer did not produce such larger species [53]. Hence, it appears that in vitro the different experimental conditions, i.e., the use of monomeric aggregating protein with respect to oligomeric species, may determine a different mode of M-TTR/oligomer interaction and suppression of oligomer toxicity. Further experimental studies are necessary to clarify this issue.

Overall, the molecular mechanism by which TTR protects cells against the deleterious effects of protein aggregation seems to involve two different levels of intervention, inhibition of protein aggregation and fibril formation, as previously demonstrated [17–21, 23, Li et al., submitted], and neutralization of protein oligomer toxicity once the oligomers are formed, as shown here. Such dual protective behavior has also been demonstrated in vitro for a number of proteins that have been widely recognized as molecular chaperones, such as αB-crystallin, Hsp70 (both with and without ATP), clusterin, α_2-macroglobulin and haptoglobin [26,57], showing that TTR can also behave as a molecule with ATP-independent chaperone activity and have a relevant functional role in vivo.

Conflict of interest

The authors declare that they have no conflict of interest.

Acknowledgements

We thank Tania Scartabelli for her technical advice. This work was supported by the Italian Ministero dell'Istruzione, dell'Universita' e della Ricerca [grant numbers PRIN2008R25HBW_002 to C.C., PRIN20083-ERXWS to F.C.] and the Fondazione Cassa di Risparmio di Pistoia e Pescia [project n. 2012.0266]. Studies from the Buxbaum Laboratory were supported by the W.M. Keck Foundation.

Appendix A. Supplementary data

Supplementary data to this article can be found online at http://dx.doi.org/10.1016/j.bbadis.2013.09.011.

References

[1] D.R. Soprano, J. Herbert, K.J. Soprano, E.A. Schon, D.S. Goodman, Demonstration of transthyretin mRNA in the brain and other extrahepatic tissues in the rat, J. Biol. Chem. 25 (1985) 11793–11798.
[2] A.J. Stauder, P.W. Dickson, A.R. Aldred, G. Schreiber, F.A. Mendelsohn, P. Hudson, Synthesis of transthyretin (pre-albumin) mRNA in choroid plexus epithelial cells, localized by in situ hybridization in rat brain, J. Histochem. Cytochem. 34 (1986) 949–952.
[3] J. Herbert, J.N. Wilcox, K.C. Pham, R.T. Fremeau, M. Zaviani, A. Dwork, D. Soprano, A. Makover, D.S. Goodman, E.Z. Zimmerman, J.L. Roberts, E.A. Schon, Transthyretin: a choroid plexus-specific transport protein in human brain, Neurology 36 (1986) 900–911.
[4] B. Jacobsson, Localization of transthyretin-mRNA and of immunoreactive transthyretin in the human fetus, Virchows Arch. A Pathol. Anat. 415 (1989) 259–263.
[5] B. Jacobsson, V.P. Collins, L. Grimelius, T. Pettersson, B. Sandstedt, A. Carlstrom, Transthyretin immunoreactivity in human and porcine liver, choroid plexus, and pancreatic islets, J. Histochem. Cytochem. 37 (1989) 31–37.
[6] T. Murakami, Y. Ohsawa, L. Zhenghua, K. Yamamura, Y. Sunada, The transthyretin gene is expressed in Schwann cells of peripheral nerves, Brain Res. 1348 (2010) 222–225.
[7] S. Wakasugi, S. Maeda, K.J. Shimada, Structure and expression of the mouse prealbumin gene, Biochemistry 100 (1986) 49–58.
[8] N. Reixach, T.R. Foss, E. Santelli, J. Pascual, J.W. Kelly, J.N. Buxbaum, Human-murine transthyretin heterotetramers are kinetically stable and non-amyloidogenic, J. Biol. Chem. 25 (2008) 2098–2107.
[9] J.N. Buxbaum, N. Reixach, Transthyretin: the servant of many masters, Cell. Mol. Life Sci. 66 (2009) 3095–3101.
[10] P. Westermark, Subcutaneous adipose tissue biopsy for amyloid protein studies, Methods Mol. Biol. 849 (2012) 363–371.
[11] M. Tanskanen, T. Peuralinna, T. Polvikoski, I.L. Notkola, R. Sulkava, J. Hardy, A. Singleton, S. Kiuru-Enari, A. Paetau, P.J. Tienari, L. Myllykangas, Senile systemic amyloidosis affects 25% of the very aged and associates with genetic variation in alpha2-macroglobulin and tau: a population-based autopsy study, Ann. Med. 40 (2008) 232–239.
[12] J.T. Lie, P.I. Hammond, Pathology of the senescent heart: anatomic observations on 237 autopsy studies of patients 90 to 105 years old, Mayo Clin. Proc. 63 (1988) 552–564.
[13] Y. Sekijima, R.L. Wiseman, J. Matteson, P. Hammarström, S.R. Miller, A.R. Sawkar, W.E. Balch, J.W. Kelly, The biological and chemical basis for tissue-selective amyloid disease, Cell 121 (2005) 73–85.
[14] F. Garzuly, R. Vidal, T. Wisniewski, F. Brittig, H. Budka, Familial meningocerebrovascular amyloidosis. Hungarian type, with mutant transthyretin (TTR Asp18Gly), Neurology 47 (1996) 1562–1567.
[15] L.H. Connors, A. Lim, T. Prokaeva, V.A. Roskens, C.E. Costello, Tabulation of 385 human transthyretin (TTR) variants, Amyloid 10 (2003) 160–184.
[16] T. Wisniewski, E. Castano, J. Ghiso, B. Frangione, Cerebrospinal fluid inhibits Alzheimer beta-amyloid fibril formation in vitro, Ann. Neurol. 34 (1993) 631–633.
[17] A.L. Schwarzman, L. Gregori, M.P. Vitek, S. Lyubski, W.J. Strittmatter, J.J. Enghilde, R. Bhasin, J. Silverman, K.H. Weisgraber, P.K. Coyle, et al., Transthyretin sequesters amyloid beta protein and prevents amyloid formation, Proc. Natl. Acad. Sci. U. S. A. 91 (1994) 8368–8372.
[18] C.D. Link, Expression of human beta-amyloid peptide in transgenic *Caenorhabditis elegans*, Proc. Natl. Acad. Sci. U. S. A. 92 (1995) 9368–9372.
[19] S.H. Choi, S.N. Leight, V.M. Lee, T. Li, P.C. Wong, J.A. Johnson, M.J. Saraiva, S.S. Sisodia, Accelerated Abeta deposition in APPswe/PS1deltaE9 mice with hemizygous deletions of TTR (transthyretin), J. Neurosci. 27 (2007) 7006–7010.
[20] J.N. Buxbaum, Z. Ye, N. Reixach, L. Friske, C. Levy, P. Das, T. Golde, E. Masliah, A.R. Roberts, T. Bartfai, Transthyretin protects Alzheimer's mice from the behavioral and biochemical effects of Abeta toxicity, Proc. Natl. Acad. Sci. U. S. A. 105 (2008) 2681–2686.
[21] L. Liu, R.M. Murphy, Kinetics of inhibition of beta-amyloid aggregation by transthyretin, Biochemistry (Mosc) 45 (2006) 15702–15709.
[22] R. Costa, A. Goncalves, M.J. Saralva, I. Cardoso, Transthyretin binding to A-beta peptide — impact on A-beta fibrillogenesis and toxicity, FEBS Lett. 582 (2008) 936–942.
[23] J. Du, R.M. Murphy, Characterization of the interaction of β-amyloid with transthyretin monomers and tetramers, Biochemistry 28 (2010) 8276–8289.
[24] J. Du, P.Y. Cho, D.T. Yang, R.M. Murphy, Identification of beta-amyloid-binding sites on transthyretin, Protein Eng. Des. Sel. 25 (2012) 337–345.
[25] X. Li, E. Masliah, N. Reixach, J.N. Buxbaum, Neuronal production of transthyretin in human and murine Alzheimer's disease: is it protective? J. Neurosci. 31 (2011) 12483–12490.
[26] B. Mannini, R. Cascella, M. Zampagni, M. van Waarde-Verhagen, S. Meehan, C. Roodveldt, S. Campioni, M. Boninsegna, A. Penco, A. Relini, H.H. Kampinga, C.M. Dobson, M.R. Wilson, C. Cecchi, F. Chiti, Molecular mechanisms used by chaperones to reduce the toxicity of aberrant protein oligomers, Proc. Natl. Acad. Sci. U. S. A. 109 (2012) 12479–12484.
[27] W. Colon, J.W. Kelly, Partial denaturation of transthyretin is sufficient for amyloid fibril formation in vitro, Biochemistry 31 (1992) 8654–8660.

[28] X. Jiang, C.S. Smith, H.M. Petrassi, P. Hammarström, J.T. White, J.C. Sacchettini, J.W. Kelly, An engineered transthyretin monomer that is nonamyloidogenic, unless it is partially denatured, Biochemistry 40 (2001) 11442–11452.
[29] S. Bourgault, S. Choi, J.N. Buxbaum, J.W. Kelly, J.L. Price, N. Reixach, Mechanisms of transthyretin cardiomyocyte toxicity inhibition by resveratrol analogs, Biochem. Biophys. Res. Commun. 410 (2011) 707–713.
[30] S. Campioni, B. Mannini, M. Zampagni, A. Pensalfini, C. Parrini, E. Evangelisti, A. Relini, M. Stefani, C.M. Dobson, C. Cecchi, F. Chiti, A causative link between the structure of aberrant protein oligomers and their ability to cause cellular dysfunction, Nat. Chem. Biol. 6 (2010) 140–147.
[31] M.P. Lambert, K.L. Viola, B.A. Chromy, L. Chang, T.E. Morgan, J. Yu, D.L. Venton, G.A. Krafft, C.E. Finch, W.L. Klein, Vaccination with soluble Abeta oligomers generates toxicity-neutralizing antibodies, J. Neurochem. 79 (2001) 595–605.
[32] J.T. White, J.W. Kelly, Support for the multigenic hypothesis of amyloidosis: the binding stoichiometry of retinol-binding protein, vitamin A, and thyroid hormone influences transthyretin amyloidogenicity in vitro, Proc. Natl. Acad. Sci. U. S. A. 98 (2001) 13019–13024.
[33] P. Hammarström, Y. Sekijima, J.T. White, R.L. Wiseman, A. Lim, C.E. Costello, K. Altland, F. Garzuly, H. Budka, J.W. Kelly, D18G transthyretin is monomeric, aggregation prone, and not detectable in plasma and cerebrospinal fluid: a prescription for central nervous system amyloidosis? Biochemistry 42 (2003) 6656–6663.
[34] A. Pensalfini, M. Zampagni, G. Liguri, M. Becatti, E. Evangelisti, C. Fiorillo, S. Bagnoli, E. Cellini, B. Nacmias, S. Sorbi, C. Cecchi, Membrane cholesterol enrichment prevents Aβ-induced oxidative stress in Alzheimer's fibroblasts, Neurobiol. Aging 32 (2011) 210–222.
[35] M. Zampagni, R. Cascella, F. Casamenti, C. Grossi, E. Evangelisti, D. Wright, M. Becatti, G. Liguri, B. Mannini, S. Campioni, F. Chiti, C. Cecchi, A comparison of the biochemical modifications caused by toxic and nontoxic protein oligomers in cells, J. Cell. Mol. Med. 15 (2011) 2106–2116.
[36] U.K. Laemmli, Cleavage of structural proteins during the assembly of the head of bacteriophage T4, Nature 227 (1970) 680–685.
[37] K. Sörgjerd, T. Klingstedt, M. Lindgren, K. Kågedal, P. Hammarström, Prefibrillar transthyretin oligomers and cold stored native tetrameric transthyretin are cytotoxic in cell culture, Biochem. Biophys. Res. Commun. 377 (2008) 1072–1078.
[38] S. Choi, N. Reixach, S. Connelly, S.M. Johnson, I.A. Wilson, J.W. Kelly, A substructure combination strategy to create potent and selective transthyretin kinetic stabilizers that prevent amyloidogenesis and cytotoxicity, J. Am. Chem. Soc. 132 (2010) 1359–1370.
[39] N. Reixach, S. Deechongkit, X. Jiang, J.W. Kelly, J.N. Buxbaum, Tissue damage in the amyloidoses: transthyretin monomers and nonnative oligomers are the major cytotoxic species in tissue culture, Proc. Natl. Acad. Sci. U. S. A. 101 (2004) 2817–2822.
[40] S. Orrenius, B. Zhovotovsky, P. Nicotera, Regulation of cell death: the calciumapoptosis link, Nat. Rev. 4 (2003) 552–565.
[41] A. Demuro, E. Mina, R. Kayed, S.C. Milton, I. Parker, C.G. Glabe, Calcium dysregulation and membrane disruption as a ubiquitous neurotoxic mechanism of soluble amyloid oligomers, J. Biol. Chem. 280 (2005) 17294–17300.
[42] C. Canale, S. Torrassa, P. Rispoli, A. Relini, R. Rolandi, M. Bucciantini, M. Stefani, A. Gliozzi, Natively folded HypF-N and its early amyloid aggregates interact with phospholipid monolayers and destabilize supported phospholipid bilayers, Biophys. J. 91 (2006) 4575–4588.
[43] L. Bojarski, J. Herms, J. Kuznicki, Calcium dysregulation in Alzheimer's disease, Neurochem. Int. 52 (2008) 621–633.
[44] E. Evangelisti, C. Cecchi, R. Cascella, C. Sgromo, M. Becatti, C.M. Dobson, F. Chiti, M. Stefani, Membrane lipid composition and its physicochemical properties define cell vulnerability to aberrant protein oligomers, J. Cell Sci. 125 (2012) 2416–2427.
[45] N.A. Thornberry, T.A. Rano, E.P. Peterson, D.M. Rasper, T. Timkey, M. Garcia-Calvo, V.M. Houtzager, P.A. Nordstrom, S. Roy, J.P. Vaillancourt, K.T. Chapman, D.W. Nicholson, A combinatorial approach defines specificities of members of the caspase family and granzyme B. Functional relationships established for key mediators of apoptosis, J. Biol. Chem. 272 (1997) 17907–17911.
[46] B. Weisblum, E. Haenssler, Fluorometric properties of the bibenzimidazole derivative Hoechst 33258, a fluorescent probe specific for AT concentration in chromosomal DNA, Chromosoma 46 (1974) 255–260.
[47] R. Cascella, S. Conti, F. Tatini, E. Evangelisti, T. Scartabelli, F. Casamenti, M.R. Wilson, F. Chiti, C. Cecchi, Extracellular chaperones prevent $A\beta_{42}$-induced toxicity in rat brains, Biochim. Biophys. Acta 1832 (2013) 1217–1226.
[48] P.N. Lacor, M.C. Buniel, L. Chang, S.J. Fernandez, Y. Gong, K.L. Viola, M.P. Lambert, P.T. Velasco, E.H. Bigio, C.E. Finch, G.A. Krafft, W.L. Klein, Synaptic targeting by Alzheimer's-related amyloid beta oligomers, J. Neurosci. 24 (2004) 10191–10200.
[49] F. Tatini, A.M. Pugliese, C. Traini, S. Niccoli, G. Maraula, T.E. Dami, B. Mannini, T. Scartabelli, F. Pedata, F. Casamenti, F. Chiti, Amyloid-β oligomer synaptotoxicity is mimicked by oligomers of the model protein HypF-N, Neurobiol. Aging (2013), http://dx.doi.org/10.1016/j.neurobiolaging.2013.03.020(S0197-4580(13)00133-4. [Epub ahead of print]).
[50] J.B. Birks, I.H. Munro, Progress in Reaction Kinetics, 4Pergamon Press, 1967.
[51] P. Hammarström, M. Persson, P.O. Freskgård, L.G. Mårtensson, D. Andersson, B.H. Jonsson, U. Carlsson, Structural mapping of an aggregation nucleation site in a molten globule intermediate, J. Biol. Chem. 274 (1999) 32897–32903.
[52] R. Krishnan, S.L. Lindquist, Structural insights into a yeast prion illuminate nucleation and strain diversity, Nature 435 (2005) 765–772.
[53] J. Ojha, G. Masilamoni, D. Dunlap, R.A. Udoff, A.G. Cashikar, Sequestration of toxic oligomers by HspB1 as a cytoprotective mechanism, Mol. Cell. Biol. 31 (2011) 3146–3157.
[54] M. Ahmed, J. Davis, D. Aucoin, T. Sato, S. Ahuja, S. Aimoto, J.I. Elliott, W.E. Van Nostrand, S.O. Smith, Structural conversion of neurotoxic amyloid-beta(1–42) oligomers to fibrils, Nat. Struct. Mol. Biol. 17 (2010) 561–567.
[55] P. Cizas, R. Budvytyte, R. Morkuniene, R. Moldovan, M. Broccio, M. Lösche, G. Niaura, G. Valincius, V. Borutaite, Size-dependent neurotoxicity of beta-amyloid oligomers, Arch. Biochem. Biophys. 496 (2010) 84–92.
[56] F. Bemporad, F. Chiti, Protein misfolded oligomers: experimental approaches, mechanism of formation, and structure–toxicity relationships, Chem. Biol. 19 (2012) 315–327.
[57] K. Sörgjerd, B. Ghafouri, B.H. Jonsson, J.W. Kelly, S.Y. Blond, P. Hammarström, Retention of misfolded mutant transthyretin by the chaperone BiP/GRP78 mitigates amyloidogenesis, J. Mol. Biol. 356 (2006) 469–482.